Oil Temperature Characterization in a Direct Suction Scroll Compressor

Nicolás Gómez Parada [1], Francisco Barceló Ruescas [1]*, José Gonzálvez Maciá [1]

[1]Universitat Politècnica de València, Instituto de Ingeniería Energética,
Valencia, Spain
energeti@upvnet.upv.es

*Corresponding Author
fbarceló@iie.upv.es

ABSTRACT

Scroll compressors are widely used on commercial and domestic heat pumps, and their main working parameters are vastly characterized and available in the literature. Nevertheless, a special constructive disposition of these compressors where suction is directly connected to the inlet of the compression mechanism and the oil sump is at the discharge conditions is not so widely characterized.

This work is focused on empirically determining the oil temperature in the sump of the compressor for a compressor with direct suction of refrigerant for a range of working conditions, including a variation of suction and discharge temperatures and compressor speed. This characterization was done in a calorimeter compressor test bench at UPV, Valencia, Spain. The refrigerant used is propane, and the oil is a PAG-type PZ46 oil. This particular compressor model is used in a commercial heat pump producing hot water for heating and domestic hot water.

The final goal will be obtaining a correlation with the proper factors in order to model the oil temperature to predict the solubility with the refrigerant and eventually obtain the refrigerant charge in the compressor. The study is engaged in a wider project consisting of implementing an upgraded charge prediction capability in a vapor compression systems simulation software. The importance of the project is related to the need to reduce the refrigerant charge used in HVAC&R systems using flammable natural refrigerants.

1. INTRODUCTION

The refrigerant and oil are typically miscible in refrigeration systems, allowing the oil to return to the compressor. However, the refrigerant-oil mixture can impact the mechanical performance by altering the thermo-physical properties of the pure oil. Lubrication plays a critical role in reducing friction, creating a hermetic seal, dissipating heat, and protecting against wear. The effectiveness of the lubricant depends primarily on its viscosity; high viscosity can reduce efficiency and cause bearing wear, while low viscosity can lead to metal-to-metal contact and insufficient sealing, also decreasing the compressor efficiency.

The solubility of the mixture determines the amount of refrigerant charge in the compressor. In this case, the tested compressor uses a mixture of PAG (Polyalkylene Glycol) oil and R-290 (Propane) as a refrigerant. The amount of propane in a system under high-pressure conditions and using PAG-type oil can represent a large portion of the total system charge, as shown in (Sánchez-Moreno-Giner et al., 2023) and (Chen et al., 2019). The refrigerant used is classified as A3 flammable. Since the charge limits of this refrigerant type are lower in domestic systems, it is essential to investigate the charge reduction of R-290 in commercial compressors.

It is vital to know the mixture's temperature to accurately estimate the viscosity and solubility of a refrigerant-oil mixture and make charge estimations. While analyses have been conducted on oil temperature for reciprocating and scroll compressors with the sump at low pressure (Navarro et al., 2012), more information is needed on scroll compressors with the oil sump at discharge pressure, The following study analyses the oil sump temperature in a high-pressure shell scroll compressor. It describes an empirical correlation that fits the experimental data, allowing initial estimations of the refrigerant charge dissolved in the oil.

2. EXPERIMENTAL SET-UP

The scroll compressor was tested on a specific test rig, as shown in Figure 1. The test rig includes a refrigerant and water loop that allows the compressor to be tested under various conditions, simulating a thermodynamic cycle. The refrigerant is condensed using a closed water loop and subcooled by an open water loop that uses brazed plate heat exchangers. Electronic expansion valves are opened to regulate the suction pressure, while resistors immersed in tanks with R134a refrigerant control the suction temperature of the compressor. The suction pressure, condensing pressure, superheat, and subcooling are all automatically controlled by PID (proportional–integral–derivative) systems.

Coriolis mass flow meters are used to measure the mass flow of refrigerant; for flow rates below 15 g/s, the Coriolis (Emerson Micro Motion CMF010) is used; for flow rates above 15 g/s, the Coriolis (Emerson Micro Motion CMF025) is used having an accuracy of 0.05% of the measured value. The accuracy of the pressure sensors (Rosemount-3051) and the temperature sensors (RTD-PT100) are 0.02% and 0.05°C, respectively.

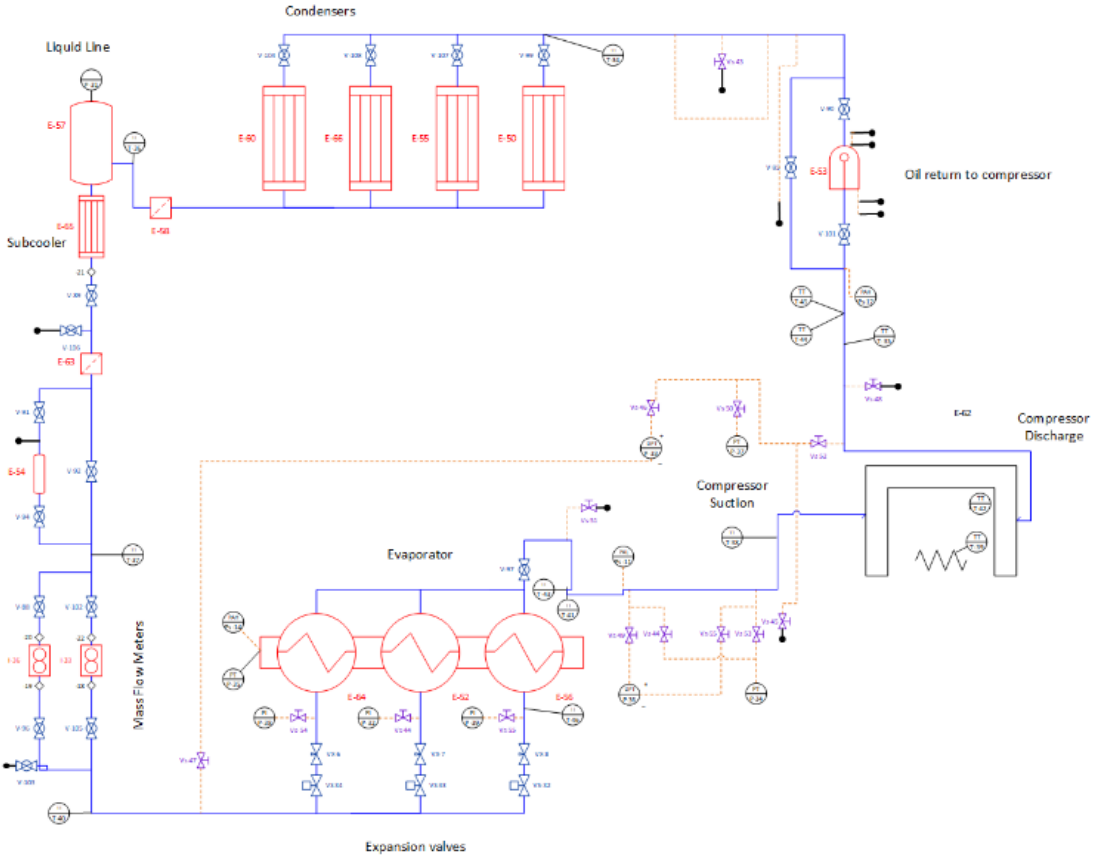

Figure 1: Experimental test rig

3. METHODOLOGY

The compressor is a direct suction scroll-type compressor. The oil carter is located at the bottom of the compressor shell, where three type-T thermocouples are situated as shown in Figure 2. These thermocouples are placed at the bottom carter and two at the carter sides. A copper isothermal block was used to measure the temperature of the oil sump, and the overall uncertainty of the oil temperature measurements was 0.5°C. It is assumed that the values measured by the thermocouples are approximately the temperature of the oil carter at a steady state. The compressor has a displacement of 52 cm3 and uses R-290 as a refrigerant. The oil used is a PAG-type PZ46M, with an oil quantity of 0.9 L, and the compressor is covered with a thermal/acoustic insulation jacket.

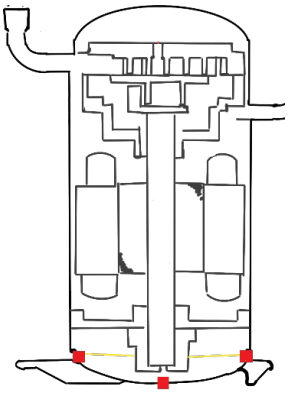

Figure 2: Scroll compressor and thermocouple locations

In this experimental arrangement, temperatures were measured when the compressor was at steady state, varying conditions from -25°C to 25 °C for the evaporating temperature and from 20°C to 82 °C for the condensing temperature. A constant superheat of 7 K was maintained for all conditions. Three compressor speeds, 30, 60, and 100 RPS, were evaluated. In some conditions, it is only possible to evaluate 30 and 60 RPS; the test matrix performed is shown in Figure 3.

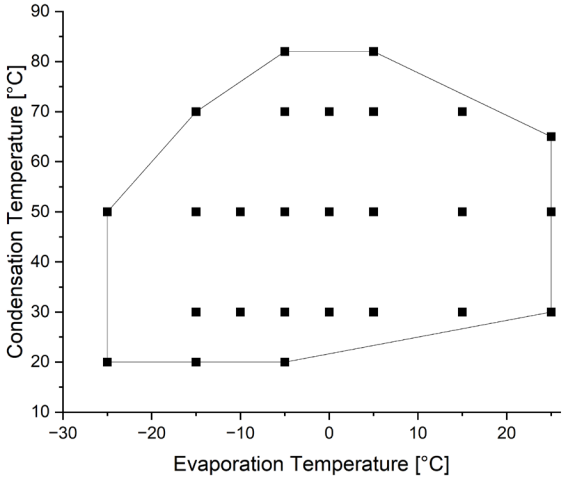

Figure 3: Test matrix

3.1 Uncertainty Analysis

Table 2 shows the systematic, random, and overall uncertainty for the nominal condition shown in Table 1.

Table 1: Nominal condition.

Condensation Temperature [°C]	Evaporation Temperature [°C]	Compressor Speed [RPS]
50	-4.7	60

Overall uncertainty is calculated from the combined standard uncertainty using the assumption of large-sample (Coleman et al., 2009):

$$U_{95} = 2u = 2\sqrt{s^2 + b^2} \quad (1)$$

Table 2: Uncertainty Analysis

Variable	Measured Data	Systematic uncertainty (95% confidence)	Random uncertainty (95% confidence)	Overall uncertainty
$P_{discharge}$	17.13 bar	±0.03 bar	±0.082 bar	±0.085 bar
$P_{suction}$	4.1 bar	±0.006 bar	±0.015 bar	±0.015 bar
$T_{discharge}$	74.53 °C	±0.07°C	±0.07 °C	±0.1 °C
$T_{suction}$	2 °C	±0.03°C	±0.06 °C	±0.07 °C
$\dot{m}_w$	25.59 g s-1	±0.02 g s-1	±0.02 g s-1	±0.04 g s-1
$\dot{E}_{comp}$ $(Inv\ included)$	2684.94 W	±5.45W	±1W	±5.84 W
$T_{bottom_{carter}}$	69.33 °C	±0.5°C	±0.02°C	±0.5ºC
$T_{side1_{carter}}$	73.94 °C	±0.5°C	±0.02°C	±0.5ºC
$T_{side2_{carter}}$	74.07 °C	±0.5°C	±0.02°C	±0.5ºC

4. RESULTS AND DISCUSSION

4.1 Experimental oil temperature and charge prediction

Analyzing the temperatures measured in the oil sump, it was observed that there was a temperature difference between the values measured at different heights. This indicates a possible stratification of the oil temperature. Figure 4 illustrates the temperature difference between the values measured at the sides of the oil carter and the temperature measured at the bottom and the lineal increase with the discharge temperature. The measurement of the sides of the oil sump is the mean value of the two thermocouples at the shell sides, since being at the same height, the values are very close.

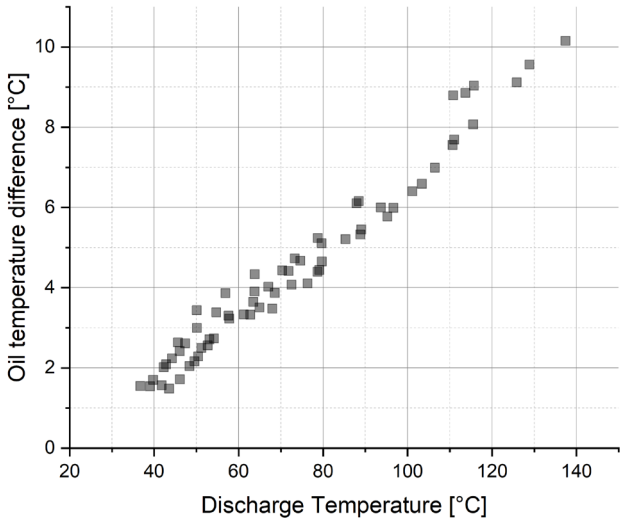

Figure 4: Oil temperature difference

Thus, the question arises as to what temperature should be used to determine the refrigerant charge. How much does this difference affect the charge estimation? To estimate the solubility, the pressure-temperature-solubility diagram usually provided by manufacturers can be used. In (Gao et al., 2019) it can be found the curve for the PZ46M/R290 oil/refrigerant mixture as shown in Figure 5; using the correlation for solubility calculation shown in the article, we calculated the solubility and estimated the amount of charge for each of the evaluated conditions.

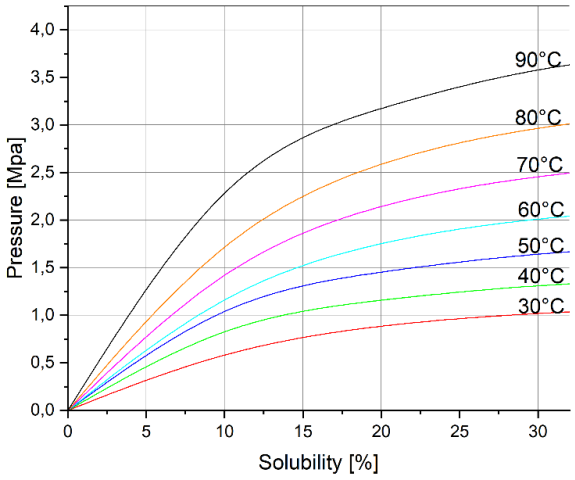

Figure 5: Saturated vapor pressure of solution versus mass concentration of R290

Solubility is defined as the ratio of the mass of refrigerant to the total mass:

$$\omega = \frac{m_{ref}}{m_{ref}+m_{oil}} \tag{2}$$

Where m_{ref} and m_{oil} are the mass of refrigerant and oil respectively. Therefore, the mass of refrigerant dissolved in the oil can be determined as follows:

$$m_{ref} = \frac{\omega * m_{oil}}{1-\omega} \tag{3}$$

Taking the volume of oil given by the manufacturer, the mass of oil is as follows:

$$m_{oil} = \rho_{oil}\, V_{oil} \tag{4}$$

The oil density of PZ46M can be describe by the following linear equation:

$$\rho_{oil} = -0.0006 * \left(Oil_{temperature}\right) + 1.0139 \tag{5}$$

Figure 6 represents the distribution of solubility calculated with the oil temperature measured at the bottom and the sides of the oil sump. In general, there is a lower solubility calculated from the temperature of the bottom of the oil sump due to the lower temperature at this location.

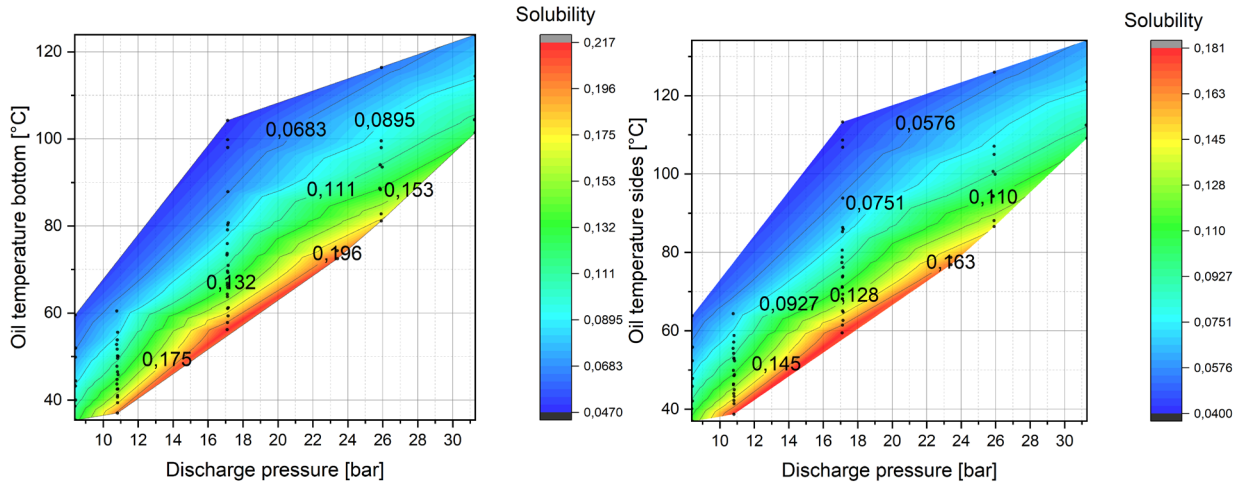

Figure 6: Estimated solubility. Left: Bottom oil sump temperature - Right: Oil sump sides mean temperature.

The maximum solubility determined from the temperature measured at the sump sides is 18.05% for the condition of 10.8 bar of discharge pressure and 38.77 °C of oil temperature. On the other hand, the maximum solubility using the bottom temperature is found at 17.1 bar pressure and 59.54 °C of oil temperature, having 21.70% solubility.

The maximum solubility did not occur at the same condition evaluated due to the temperature difference of the oil; at the same condition as the maximum solubility using the sump bottom temperature, the sump side temperature is higher by 3.3 °C; this temperature difference reduces the solubility saturation to 17.97%.

Figure 7 represents the amount of refrigerant dissolved in oil estimated from the different oil temperatures measured. The charge corresponding to the previously mentioned conditions of maximum solubility is 244.5 g, calculated with the temperature of the bottom of the oil sump and 196.11g estimated from the temperature of the sides. This represents a difference in charge estimation of 48.39g in the refrigerant dissolved in the oil, an increase of about 25% of the estimated charge, which represents a sensitive amount when designing low-charge systems; on average, there is a difference of 18.75g less charge if it is calculated from the oil temperature of the sides of the oil sump and the maximum charge difference founded is around 54.15g, and the minimum is 5.66g.

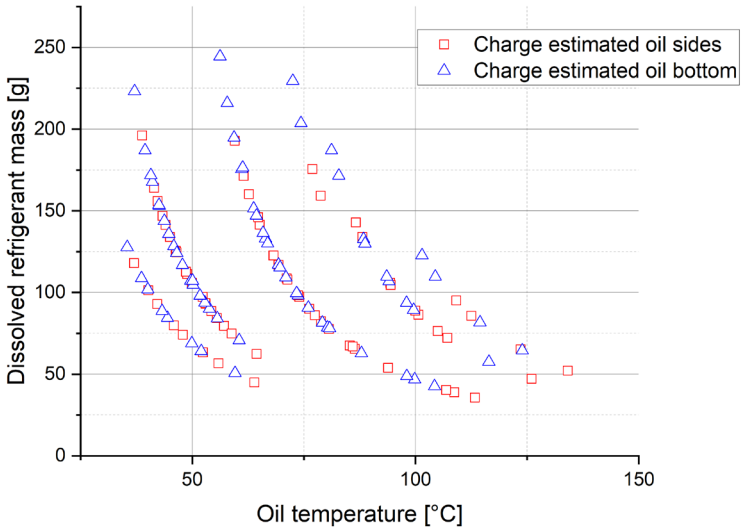

Figure 7: Predicted mass of R290 from different oil temperature measurements.

In (Shi et al., 2022), the lubricant in a rotary compressor with R290 is analyzed to understand its behavior under high-pressure conditions. Although the topology of the compressor is different, the study sheds light on the subject. The researchers used two viscometers located at different heights inside the oil sump and also measured two different temperatures. Using the measurements obtained from the viscometers and the PVTS (Pressure-Viscosity-Temperature-Solubility) diagram for the refrigerant-oil mixture, the researchers were able to calculate the actual solubility at the two measured points, which were found to be almost equal. Furthermore, they found that the saturated solubility calculated with the PTS (Pressure-Temperature-Solubility) diagram at the temperature measured at the top of the sump was close to the actual solubility of the mixture. Therefore, in the present study, the actual oil temperature should be referred to as the temperature measured at the sides of the oil carter instead of at the bottom while following this approach.

4.2 Oil correlation

Figure 8on the left shows the oil sump temperature measured at the sides versus the pressure ratio for different compressor speeds. The figure shows a difference that depends mainly on the condensation temperature. Also, with an increase in pressure ratio and compressor speed, the oil temperature also increases for the same condensation temperature. The graph on the right side of Figure 8depicts the discharge temperature in relation to the pressure ratio. It exhibits a similar trend to that of the oil temperature; the discharge temperatures show a minor deviation from the oil temperatures, indicating a close correlation between the two.

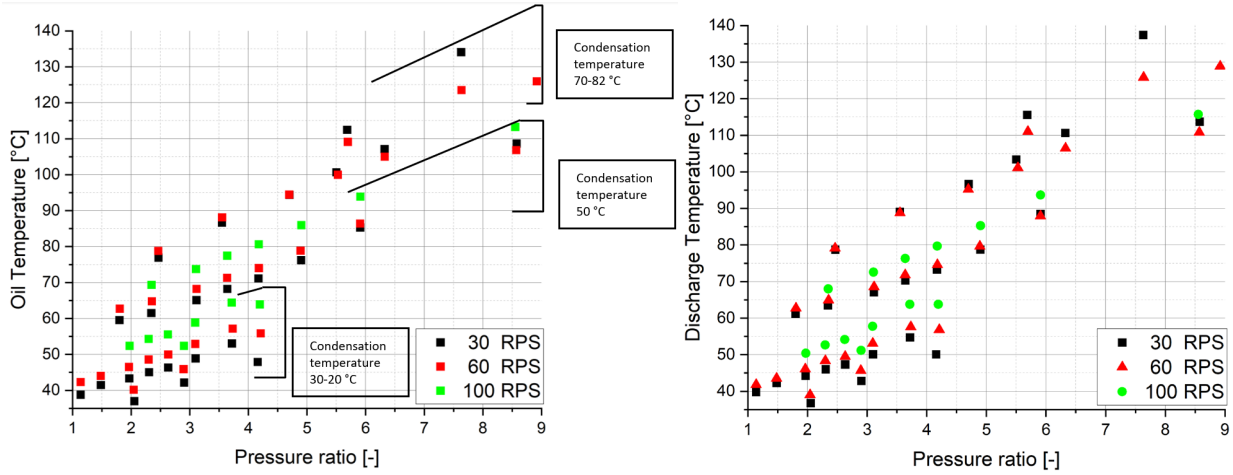

Figure 8: Left: Oil temperature vs Pressure ratio - Right: Discharge temperature vs Pressure ratio

It has been observed that at high compression ratios, there is a change in the trend. In such cases, the oil temperature of 30 RPS is either close to or higher than the oil temperature of 60 RPS under the same conditions. This may be due to the increased compressor work and reduced oil flow at low speeds, which results in higher compressor heat losses and discharge temperatures, leading to an increase in oil temperature. In order to correlate the oil temperature to the discharge temperature and its variation with the compressor speed and pressure ratio, an empirical correlation is proposed as shown in Equation 5, being the temperature in Celsius (°C) and the compressor speed in revolutions per second (RPS):

$$T_{carter} = C_1 T_{dis} + C_2 Pr + C_3 Cspeed \tag{5}$$

The correlation coefficients are shown in Table 3; as seen during the analysis, the oil temperature depends mainly on the discharge temperature. The linear correlation can predict the oil temperature with a deviation of less than 1°C for all tested points with a mean error of 0.47 °C. Figure 9 shows the comparison between the experimental and correlated values.

Table 3: Correlation coefficients

C1	C2	C3	Multiple correlation coefficient	Mean error
0.9799±0.0039	-0.3472±0.063	0.0349±0.0018	0.999	0.4758

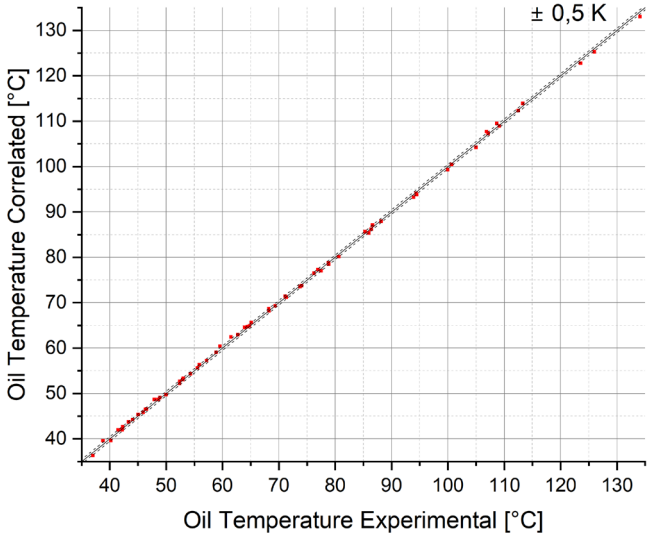

Figure 9: Oil temperature correlation comparison

Figure 10 compares the amount of refrigerant charge dissolved in the oil calculated from the experimental measurements and the correlated temperatures. The difference in the calculated charge remains within an error of less than 10% for all conditions to be evaluated, with a maximum error of 5.67% and an average error of 1.44%.

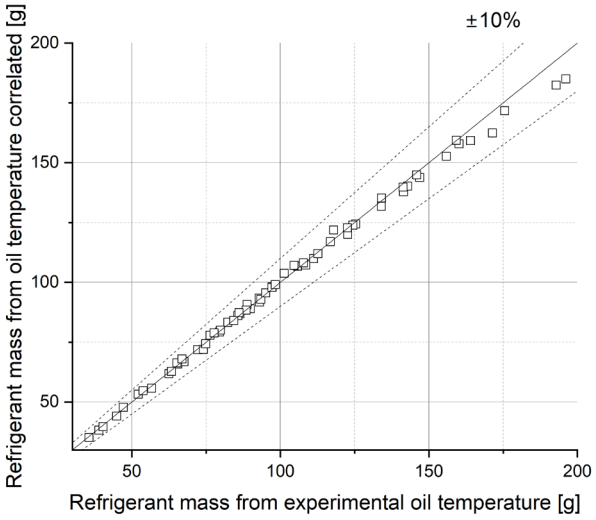

Figure 10: Refrigerant mass deviation predicted from oil temperature correlation

In the conditions corresponding to regions of higher solubility, i.e., regions of low temperature and pressures above 10 bar, a temperature difference of about 0.8 °C can represent charge differences of up to 11g, so to obtain a reliable charge prediction, it is necessary to get an accurate temperature prediction, especially under those conditions.

The amount of refrigerant dissolved in the maximum solubility condition is 196.1 g, estimated from the experimentally measured temperature, and 185g, estimated from the correlation for the oil temperature. The amount of charge dissolved in this condition (Tcond=30°C, Tevap=25, 30RPS) is important considering that this compressor is designed for a heat pump system with 1300g of propane, representing about 15% of the total charge and this only taking into account the refrigerant dissolved in the oil.

On the other hand, it is essential to note that the viscosity of the oil/refrigerant mixture depends strongly on the solubility and the change in the viscosity of the pure oil at a given temperature. The change in the lubrication properties affects the system's mechanical performance, which is a subject that has to be further analyzed in this type of compressor.

This first analysis is part of a larger project to make accurate charge predictions in a vapor compression cycle simulation software. The next step will be to be able to do an oil temperature analysis in a non-isolated system and under different ambient temperatures. Future charge extraction tests should be developed to validate the charge predictions of the proposed models.

5. CONCLUSIONS

In the present work, the oil sump temperature was analyzed in a direct suction compressor under different conditions, and a preliminary prediction of the refrigerant charge dissolved in the oil was made. The following conclusions are obtained:

- The oil sump temperature is not uniform in any condition. The temperature of the bottom of the oil sump is lower than that of the sides, with differences of up to 10 K.
- Correctly determining the temperature in the oil sump is an important factor in determining the solubility of the refrigerant in oil; differences of around 3.3 ° C may involve charge differences of more than 50g in the compressor tested for specific conditions.

- A linear correlation based on the discharge temperature, pressure ratio, and compressor speed can accurately fit the experimental data with a mean error of only 0.47. This correlation enables predicting the oil temperature of the tested compressor with a maximum error of 1°C.
- Under certain conditions of low oil temperature and high pressure, temperature errors of about 0.8 °C can give an error in the predicted charge of about 11g.
- Experimental charge extraction tests on the compressor will be necessary to validate the proposed charge prediction models.

REFERENCES

Chen, R., Wu, J., & Duan, J. (2019). Performance and refrigerant mass distribution of a R290 split air conditioner with different lubricating oils. *Applied Thermal Engineering*, *162*. https://doi.org/10.1016/j.applthermaleng.2019.114225

Coleman, H. W., Steele, W. Glenn., & Coleman, H. W. (2009). *Experimentation, validation, and uncertainty analysis for engineers*. John Wiley & Sons.

Gao, Y., He, G., Chen, P., Zhao, X., & Cai, D. (2019). Energy and exergy analysis of an air-cooled waste heat-driven absorption refrigeration cycle using R290/oil as working fluid. *Energy*, *173*, 820–832. https://doi.org/10.1016/j.energy.2019.02.117

Navarro, E., Corberán, J. M., Martínez-Galvan, I. O., & Gonzálvez, J. (2012). Oil sump temperature in hermetic compressors for heat pump applications. *International Journal of Refrigeration*, *35*(2), 397–406. https://doi.org/10.1016/j.ijrefrig.2011.10.006

Sánchez-Moreno-Giner, L., Methler, T., Barceló-Ruescas, F., & Gonzálvez-Maciá, J. (2023). Refrigerant charge distribution in brine-to-water heat pump using R290 as refrigerant. *International Journal of Refrigeration*, *145*, 158–167. https://doi.org/10.1016/j.ijrefrig.2022.10.013

Shi, H., Lei, B., & Wu, J. (2022). Lubrication of R290 Rotary Compressor Used in Low-Temperature Air-Water Heat Pumps. *International Journal of Refrigeration*, *144*, 163–174. https://doi.org/10.1016/j.ijrefrig.2022.07.007

ACKNOWLEDGEMENT

The work of Nicolás Gómez Parada in this project has been partially supported by Generalitat Valenciana, under the program Santiago Grisolía with reference GRISOLIAP/2021/084. The authors would like to acknowledge the Spanish "MINISTERIO DE CIENCIA E INNOVACIÓN", through the project ref-PID2020–115665RB-I00 "Descarbonización de Edificios e Industrias con sistemas híbridos de bomba de Calor" for the given support.